Search for charged Higgs bosons in e^+e^- collisions at energies up to $\sqrt{s} = 209$ GeV

A. Heister, S. Schael, R. Barate, R. Bruneliere, I. de Bonis, D. Decamp, C. Goy, S. Jezequel, J P. Lees, F. Martin, et al.

EUROPEAN ORGANIZATION FOR NUCLEAR RESEARCH

CERN EP/2002-054
11-July-2002

Search for charged Higgs bosons in e^+e^- collisions at energies up to $\sqrt{s} = 209$ GeV

The ALEPH Collaboration*)

Abstract

A search for charged Higgs bosons produced in pairs is performed with data collected at centre-of-mass energies ranging from 189 to 209 GeV by ALEPH at LEP, corresponding to a total luminosity of 629 pb^{-1}. The three final states $\tau^+\nu_\tau\tau^-\bar{\nu}_\tau$, $\mathrm{c\bar{s}}\tau^-\bar{\nu}_\tau$ and $\mathrm{c\bar{s}s\bar{c}}$ are considered. No evidence for a signal is found and lower limits are set on the mass $m_{\mathrm{H}^\pm}$ as a function of the branching fraction $\mathrm{B}(\mathrm{H}^+ \to \tau^+\nu_\tau)$. In the framework of a two-Higgs-doublet model, and assuming $\mathrm{B}(\mathrm{H}^+ \to \tau^+\nu_\tau)+\mathrm{B}(\mathrm{H}^+ \to \mathrm{c\bar{s}})=1$, charged Higgs bosons with masses below 79.3 GeV/c^2 are excluded at 95% confidence level independently of the branching ratios.

(Submitted to Physics Letters B)

---

*) See next pages for the list of authors

The ALEPH Collaboration

A. Heister, S. Schael

Physikalisches Institut das RWTH-Aachen, D-52056 Aachen, Germany

R. Barate, R. Brunelière, I. De Bonis, D. Decamp, C. Goy, S. Jezequel, J.-P. Lees, F. Martin, E. Merle, M.-N. Minard, B. Pietrzyk, B. Trocmé

Laboratoire de Physique des Particules (LAPP), IN^{2}P^3-CNRS, F-74019 Annecy-le-Vieux Cedex, France

G. Boix,[25] S. Bravo, M.P. Casado, M. Chmeissani, J.M. Crespo, E. Fernandez, M. Fernandez-Bosman, Ll. Garrido,[15] E. Graugés, J. Lopez, M. Martinez, G. Merino, A. Pacheco, D. Paneque, H. Ruiz

Institut de Física d'Altes Energies, Universitat Autònoma de Barcelona, E-08193 Bellaterra (Barcelona), Spain[7]

A. Colaleo, D. Creanza, N. De Filippis, M. de Palma, G. Iaselli, G. Maggi, M. Maggi, S. Nuzzo, A. Ranieri, G. Raso,[24] F. Ruggieri, G. Selvaggi, L. Silvestris, P. Tempesta, A. Tricomi,[3] G. Zito

Dipartimento di Fisica, INFN Sezione di Bari, I-70126 Bari, Italy

X. Huang, J. Lin, Q. Ouyang, T. Wang, Y. Xie, R. Xu, S. Xue, J. Zhang, L. Zhang, W. Zhao

Institute of High Energy Physics, Academia Sinica, Beijing, The People's Republic of China[8]

D. Abbaneo, P. Azzurri, T. Barklow,[30] O. Buchmüller,[30] M. Cattaneo, F. Cerutti, B. Clerbaux,[23] H. Drevermann, R.W. Forty, M. Frank, F. Gianotti, T.C. Greening,[26] J.B. Hansen, J. Harvey, D.E. Hutchcroft, P. Janot, B. Jost, M. Kado,[2] P. Mato, A. Moutoussi, F. Ranjard, L. Rolandi, D. Schlatter, G. Sguazzoni, W. Tejessy, F. Teubert, A. Valassi, I. Videau, J.J. Ward

European Laboratory for Particle Physics (CERN), CH-1211 Geneva 23, Switzerland

F. Badaud, S. Dessagne, A. Falvard,[20] D. Fayolle, P. Gay, J. Jousset, B. Michel, S. Monteil, D. Pallin, J.M. Pascolo, P. Perret

Laboratoire de Physique Corpusculaire, Université Blaise Pascal, IN^{2}P^3-CNRS, Clermont-Ferrand, F-63177 Aubière, France

J.D. Hansen, J.R. Hansen, P.H. Hansen, B.S. Nilsson

Niels Bohr Institute, 2100 Copenhagen, DK-Denmark[9]

A. Kyriakis, C. Markou, E. Simopoulou, A. Vayaki, K. Zachariadou

Nuclear Research Center Demokritos (NRCD), GR-15310 Attiki, Greece

A. Blondel,[12] J.-C. Brient, F. Machefert, A. Rougé, M. Swynghedauw, R. Tanaka H. Videau

Laoratoire Leprince-Ringuet, Ecole Polytechnique, IN^{2}P^3-CNRS, F-91128 Palaiseau Cedex, France

V. Ciulli, E. Focardi, G. Parrini

Dipartimento di Fisica, Università di Firenze, INFN Sezione di Firenze, I-50125 Firenze, Italy

A. Antonelli, M. Antonelli, G. Bencivenni, F. Bossi, G. Capon, V. Chiarella, P. Laurelli, G. Mannocchi,[5] G.P. Murtas, L. Passalacqua

Laboratori Nazionali dell'INFN (LNF-INFN), I-00044 Frascati, Italy

J. Kennedy, J.G. Lynch, P. Negus, V. O'Shea, A.S. Thompson

Department of Physics and Astronomy, University of Glasgow, Glasgow G12 8QQ,United Kingdom[10]

S. Wasserbaech

Department of Physics, Haverford College, Haverford, PA 19041-1392, U.S.A.

R. Cavanaugh,[4] S. Dhamotharan,[21] C. Geweniger, P. Hanke, V. Hepp, E.E. Kluge, G. Leibenguth, A. Putzer, H. Stenzel, K. Tittel, M. Wunsch[19]

Kirchhoff-Institut für Physik, Universität Heidelberg, D-69120 Heidelberg, Germany[16]

R. Beuselinck, W. Cameron, G. Davies, P.J. Dornan, M. Girone,[1] R.D. Hill, N. Marinelli, J. Nowell, S.A. Rutherford, J.K. Sedgbeer, J.C. Thompson,[14] R. White

Department of Physics, Imperial College, London SW7 2BZ, United Kingdom[10]

V.M. Ghete, P. Girtler, E. Kneringer, D. Kuhn, G. Rudolph

Institut für Experimentalphysik, Universität Innsbruck, A-6020 Innsbruck, Austria[18]

E. Bouhova-Thacker, C.K. Bowdery, D.P. Clarke, G. Ellis, A.J. Finch, F. Foster, G. Hughes, R.W.L. Jones, M.R. Pearson, N.A. Robertson, M. Smizanska

Department of Physics, University of Lancaster, Lancaster LA1 4YB, United Kingdom[10]

O. van der Aa, C. Delaere, V. Lemaitre

Institut de Physique Nucléaire, Département de Physique, Université Catholique de Louvain, 1348 Louvain-la-Neuve, Belgium

U. Blumenschein, F. Hölldorfer, K. Jakobs, F. Kayser, K. Kleinknecht, A.-S. Müller, G. Quast,[6] B. Renk, H.-G. Sander, S. Schmeling, H. Wachsmuth, C. Zeitnitz, T. Ziegler

Institut für Physik, Universität Mainz, D-55099 Mainz, Germany[16]

A. Bonissent, P. Coyle, C. Curtil, A. Ealet, D. Fouchez, P. Payre, A. Tilquin

Centre de Physique des Particules de Marseille, Univ Méditerranée, IN^{2}P^3-CNRS, F-13288 Marseille, France

F. Ragusa

Dipartimento di Fisica, Università di Milano e INFN Sezione di Milano, I-20133 Milano, Italy.

A. David, H. Dietl, G. Ganis,[27] K. Hüttmann, G. Lütjens, W. Männer, H.-G. Moser, R. Settles, G. Wolf

Max-Planck-Institut für Physik, Werner-Heisenberg-Institut, D-80805 München, Germany[16]

J. Boucrot, O. Callot, M. Davier, L. Duflot, J.-F. Grivaz, Ph. Heusse, A. Jacholkowska,[32] L. Serin, J.-J. Veillet, J.-B. de Vivie de Régie,[28] C. Yuan

Laboratoire de l'Accélérateur Linéaire, Université de Paris-Sud, IN^{2}P^3-CNRS, F-91898 Orsay Cedex, France

G. Bagliesi, T. Boccali, L. Foà, A. Giammanco, A. Giassi, F. Ligabue, A. Messineo, F. Palla, G. Sanguinetti, A. Sciabà, R. Tenchini,[1] A. Venturi,[1] P.G. Verdini

Dipartimento di Fisica dell'Università, INFN Sezione di Pisa, e Scuola Normale Superiore, I-56010 Pisa, Italy

O. Awunor, G.A. Blair, G. Cowan, A. Garcia-Bellido, M.G. Green, L.T. Jones, T. Medcalf, A. Misiejuk, J.A. Strong, P. Teixeira-Dias

Department of Physics, Royal Holloway & Bedford New College, University of London, Egham, Surrey TW20 OEX, United Kingdom[10]

R.W. Clifft, T.R. Edgecock, P.R. Norton, I.R. Tomalin

Particle Physics Dept., Rutherford Appleton Laboratory, Chilton, Didcot, Oxon OX11 OQX, United Kingdom[10]

B. Bloch-Devaux, D. Boumediene, P. Colas, B. Fabbro, E. Lançon, M.-C. Lemaire, E. Locci, P. Perez, J. Rander, P. Seager, B. Tuchming, B. Vallage

CEA, DAPNIA/Service de Physique des Particules, CE-Saclay, F-91191 Gif-sur-Yvette Cedex, France[17]

N. Konstantinidis, A.M. Litke, G. Taylor

Institute for Particle Physics, University of California at Santa Cruz, Santa Cruz, CA 95064, USA[22]

C.N. Booth, S. Cartwright, F. Combley,[31] P.N. Hodgson, M. Lehto, L.F. Thompson
Department of Physics, University of Sheffield, Sheffield S3 7RH, United Kingdom[10]

A. Böhrer, S. Brandt, C. Grupen, J. Hess, A. Ngac, G. Prange, U. Sieler
Fachbereich Physik, Universität Siegen, D-57068 Siegen, Germany[16]

C. Borean, G. Giannini
Dipartimento di Fisica, Università di Trieste e INFN Sezione di Trieste, I-34127 Trieste, Italy

H. He, J. Putz, J. Rothberg
Experimental Elementary Particle Physics, University of Washington, Seattle, WA 98195 U.S.A.

S.R. Armstrong, K. Berkelman, K. Cranmer, D.P.S. Ferguson, Y. Gao,[29] S. González, O.J. Hayes, H. Hu, S. Jin, J. Kile, P.A. McNamara III, J. Nielsen, Y.B. Pan, J.H. von Wimmersperg-Toeller, W. Wiedenmann, J. Wu, Sau Lan Wu, X. Wu, G. Zobernig
Department of Physics, University of Wisconsin, Madison, WI 53706, USA[11]

G. Dissertori
Institute for Particle Physics, ETH Hönggerberg, 8093 Zürich, Switzerland.

[1]Also at CERN, 1211 Geneva 23, Switzerland.
[2]Now at Fermilab, PO Box 500, MS 352, Batavia, IL 60510, USA
[3]Also at Dipartimento di Fisica di Catania and INFN Sezione di Catania, 95129 Catania, Italy.
[4]Now at University of Florida, Department of Physics, Gainesville, Florida 32611-8440, USA
[5]Also Istituto di Cosmo-Geofisica del C.N.R., Torino, Italy.
[6]Now at Institut für Experimentelle Kernphysik, Universität Karlsruhe, 76128 Karlsruhe, Germany.
[7]Supported by CICYT, Spain.
[8]Supported by the National Science Foundation of China.
[9]Supported by the Danish Natural Science Research Council.
[10]Supported by the UK Particle Physics and Astronomy Research Council.
[11]Supported by the US Department of Energy, grant DE-FG0295-ER40896.
[12]Now at Departement de Physique Corpusculaire, Université de Genève, 1211 Genève 4, Switzerland.
[13]Supported by the Commission of the European Communities, contract ERBFMBICT982874.
[14]Supported by the Leverhulme Trust.
[15]Permanent address: Universitat de Barcelona, 08208 Barcelona, Spain.
[16]Supported by Bundesministerium für Bildung und Forschung, Germany.
[17]Supported by the Direction des Sciences de la Matière, C.E.A.
[18]Supported by the Austrian Ministry for Science and Transport.
[19]Now at SAP AG, 69185 Walldorf, Germany
[20]Now at Groupe d' Astroparticules de Montpellier, Université de Montpellier II, 34095 Montpellier, France.
[21]Now at BNP Paribas, 60325 Frankfurt am Mainz, Germany
[22]Supported by the US Department of Energy, grant DE-FG03-92ER40689.
[23]Now at Institut Inter-universitaire des hautes Energies (IIHE), CP 230, Université Libre de Bruxelles, 1050 Bruxelles, Belgique
[24]Also at Dipartimento di Fisica e Tecnologie Relative, Università di Palermo, Palermo, Italy.
[25]Now at McKinsey and Compagny, Avenue Louis Casal 18, 1203 Geneva, Switzerland.
[26]Now at Honeywell, Phoenix AZ, U.S.A.
[27]Now at INFN Sezione di Roma II, Dipartimento di Fisica, Università di Roma Tor Vergata, 00133 Roma, Italy.
[28]Now at Centre de Physique des Particules de Marseille, Univ Méditerranée, F-13288 Marseille, France.
[29]Also at Department of Physics, Tsinghua University, Beijing, The People's Republic of China.
[30]Now at SLAC, Stanford, CA 94309, U.S.A.
[31]Deceased.
[32]Also at Groupe d' Astroparticules de Montpellier, Université de Montpellier II, 34095 Montpellier, France.

1 Introduction

The Standard Model of electroweak interactions requires only one doublet of complex scalar fields, resulting in a single neutral Higgs particle. The simplest extensions of the Standard Model assume two complex scalar-field doublets, with a total of eight degrees of freedom. As in the Standard Model, three of the degrees of freedom are associated with the longitudinal components of the $W^{\pm}$ and Z bosons. The remaining five degrees of freedom appear as five physical scalar Higgs states: three neutral Higgs bosons and the charged Higgs bosons $H^{\pm}$.

In the two-Higgs-doublet case, the charged Higgs boson couplings are completely specified in terms of the electric charge and the weak mixing angle θ_W. The production cross-section thus depends only on the mass $m_{H^{\pm}}$. For masses accessible at LEP 2 energies, the charged Higgs boson decays with negligible lifetime and width into either $c\bar{s}/\bar{c}b$ or $\tau^+\nu_\tau$ final states. Because the analyses are not sensitive to the quark flavour, and because the $c\bar{s}$ decay mode dominates over $\bar{c}b$, $c\bar{s}$ stands for either $c\bar{s}$ or $\bar{c}b$ in the following. Therefore, $B(H^+ \to \tau^+\nu_\tau)+B(H^+ \to c\bar{s})=1$ is assumed and H^+H^- pair production leads to three final states ($\tau^+\nu_\tau\tau^-\bar{\nu}_\tau$, $c\bar{s}\tau^-\bar{\nu}_\tau/\bar{c}s\tau^+\nu_\tau$ and $c\bar{s}s\bar{c}$) for which separate searches are performed.

The ALEPH data collected at energies up to 189 GeV have already been analysed and the search results published in Refs. [1, 2, 3]. The negative result of the search, under the hypotheses specified above, was translated into a lower limit on the $H^{\pm}$ mass of 65.5 GeV/c^2 at 95% confidence level (C.L.). Results from other experiments are given in Ref. [4]. The present letter describes the search for pair-produced charged Higgs bosons using the data collected up to the end of data taking. An improved analysis has been designed for the fully leptonic channel. In the semileptonic search, the rejection of the W^+W^- background has been refined with a method based on a combination of the charge-tagged boson production angle and a τ polarization estimator. For the four-jet event selection, the linear discriminant analysis (LDA) has been re-optimized to account for the additional integrated luminosity collected at increased centre-of-mass energies.

2 The ALEPH detector and event samples

A complete and detailed description of the ALEPH detector and its performance, as well as of the standard reconstruction and analysis algorithms can be found in Refs. [5, 6]. Only those items relevant for the final states under study in this letter are summarized below.

The trajectories of the charged particles (called *charged tracks* in the following) are measured with the central tracking system, formed by a silicon vertex detector, an inner drift chamber and a large time projection chamber, all immersed in the 1.5 T axial magnetic field from a superconducting solenoidal coil. Electrons and photons are identified in the electromagnetic calorimeter, a highly segmented sampling calorimeter placed between the tracking device and the coil. Muons are identified in the hadron calorimeter, a 1.2 m thick iron yoke instrumented with 23 layers of streamer tubes, surrounded with two double layers of muon chambers. Together with the luminometers, the hermetic calorimetric coverage

extends down to 34 mrad of the beam axis. The missing energy and momentum from, *e.g.*, tau charged Higgs boson decays, are determined with an energy-flow algorithm which combines particle identification, tracking and calorimetry information into a set of energy-flow particles, used in the present analyses.

The data analysed in this letter were collected at LEP between 1998 and 2000 at e^+e^- centre-of-mass energies ranging from 189 to 209 GeV, corresponding to a total integrated luminosity of 629 pb^{-1}. The details for each sample are given in Table 1.

Table 1: Integrated luminosities, centre-of-mass energy ranges and mean centre-of-mass energy values for the data collected with the ALEPH detector from 1998 to 2000.

Year	Luminosity (pb^{-1})	Energy range (GeV)	$\langle\sqrt{s}\rangle$ (GeV)
2000	217.2	$204-209$	206.1
1999	42.0	–	201.6
	86.3	–	199.5
	79.8	–	195.5
	28.9	–	191.6
1998	174.4	–	188.6

Fully simulated samples of events reconstructed with the same programs as the data were used for the background estimates, the design of the selections and the optimization of the selection cuts. The most important background sources are *(i)* difermion events ($e^+e^- \to \tau^+\tau^-$ and $q\bar{q}$) simulated with the KORALZ [7] generator; and *(ii)* $e^+e^- \to W^+W^-$ and other four-fermion processes simulated with the KORALW [8] and PYTHIA [9] generators. Event samples of these background processes, corresponding to at least 20 times the collected luminosity, were generated. The W^+W^- cross sections predicted by RACOONWW [10] and YFSWW [11] were used as discussed in Ref. [12]. Finally, the two-photon interactions ($\gamma\gamma \to$ leptons) were simulated with the PHOT02 [13] generator. Samples of these events with at least six times the collected luminosity were generated.

The signal events generated with the HZHA [14] program were simulated for each of the final states and centre-of-mass energies (Table 1), and for charged Higgs boson masses between 45 and 100 GeV/c^2.

3 Analyses

An event selection has been defined for each of the $\tau^+\nu_\tau\tau^-\bar{\nu}_\tau$, $c\bar{s}\tau^-\bar{\nu}_\tau/\bar{c}s\tau^+\nu_\tau$ (hereafter referred to as $c\bar{s}\tau^-\bar{\nu}_\tau$) and $c\bar{s}s\bar{c}$ channels, and was optimized for $B(H^+ \to \tau^+\nu_\tau) = 100\%$, 50% and 0%, respectively. The selection criteria were chosen to achieve the highest 95% confidence level expected limit on the charged Higgs boson mass in the absence of signal.

3.1 The $\tau^+\nu_\tau\tau^-\bar{\nu}_\tau$ final state

Events with two to six charged tracks (at least one and at most four of each sign) are considered. Leptonic events $\mathrm{W^+W^-} \to \ell\nu\ell'\bar{\nu}$ ($\ell, \ell' = \mathrm{e}$ or μ) are rejected by requiring that the momentum of any identified electron or muon be less than $0.1\sqrt{s}$. The events are then forced to form two jets with the JADE algorithm [15]. An event is selected if both jet polar angles $\theta_{1,2}$ satisfy $|\cos\theta_{1,2}| < 0.96$, if their reconstructed masses are less than $3\,\mathrm{GeV}/c^2$ and if each jet contains at least one charged track. To suppress the high cross section $\gamma\gamma \to \mathrm{f\bar{f}}$ processes, the total visible mass is required to be in excess of $0.075\sqrt{s}$, the momentum transverse to the beam is required to be greater than $10\,\mathrm{GeV}/c$, and there must be no energy deposited in a cone of 12° around the beam axis. The signal selection efficiency of the latter cut is corrected for the effect of the beam-related background, not included in the simulation, and is estimated from events triggered at random beam crossings. The relative loss of signal efficiency is about 7%.

Nearly coplanar tau pairs from $\mathrm{e^+e^-} \to \tau^+\tau^-(\gamma)$ are rejected by requiring that the angle α between the two tau jets be less than 170° and the angle between the projections of their momenta onto the plane transverse to the beam axis be less than 165°. The missing energy is required to be greater than 80 GeV and the missing mass greater than $70\,\mathrm{GeV}/c^2$. In order to improve the $\mathrm{W^+W^-}$ background rejection, an LDA has been used to construct a discriminant variable D_0 from a combination of the following four quantities:

- a charge-tagged angular variable calculated from the polar angles of the τ jets and their charges as $C = \frac{1}{2}\,[\,Q_1\cos\theta_1 + Q_2\cos\theta_2\,]$;
- the angle α between the two tau jets;
- the missing transverse momentum of the event P_T^{miss};
- the value y_{23} of the jet-clustering resolution parameter for which the transition from two to three jets occurs.

The optimal discriminant variable was found to be

$$D_0 \;=\; 0.930\;C \;-\; 0.250\;\alpha \;+\; 0.008\;P_T^{\mathrm{miss}} \;-\; 110\;y_{23} \;+\; 0.426\;,$$

where α is in radians and P_T^{miss} in GeV/c. The distribution of D_0 is displayed in Fig. 1. This quantity is used as a discriminant variable in the derivation of the mass limit.

The signal event selection efficiencies, parametrized as a function of $m_{\mathrm{H^\pm}}$, are given in Table 2 for $\sqrt{s} = 206\,\mathrm{GeV}$. The selection efficiencies are almost independent of the centre-of-mass energy and increase only slightly with $m_{\mathrm{H^\pm}}$. For a signal with $m_{\mathrm{H^\pm}}$=$85\,\mathrm{GeV}/c^2$ and $\mathrm{B(H^+ \to \tau^+\nu_\tau)}$=1, a total of 16.5 events is expected in the data taken at centre-of-mass energies between 189 GeV and 209 GeV. The numbers of events selected are given in Table 3, compared to the expectations from the Standard Model backgrounds, dominated by $\mathrm{W^+W^-}$ production.

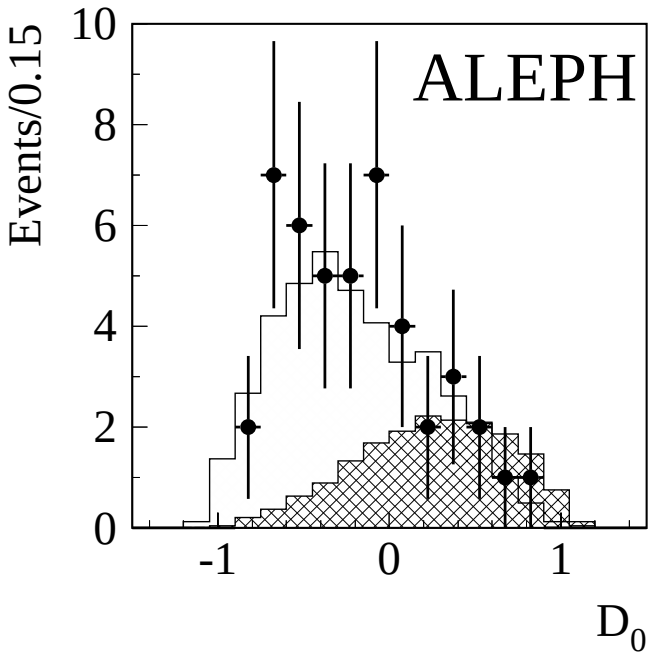

Figure 1: The distribution of the discriminant variable D_0 described in the text for the fully-leptonic channel. The points are the data, the open histogram is the Standard Model background and the hatched histogram represents the Higgs signal expectation, absolutely normalized, with $m_{\mathrm{H}^\pm} = 85\,\mathrm{GeV}/c^2$.

The systematic uncertainty on the number of expected signal events is estimated to be 3.1%, dominated by the effect of limited Monte Carlo statistics (2.4%) and the uncertainty on the cross section for charged Higgs boson production (2%). The systematic error on the background level is estimated to be 1.5%, dominated by the effects of limited Monte Carlo statistics (1.3%), by the uncertainty on the cross section for the $\mathrm{W}^+\mathrm{W}^-$ process (0.5%) and the uncertainty on the cross section for two-photon production (5%).

3.2 The $\mathrm{c\bar{s}}\tau^-\bar{\nu}_\tau$ final state

The mixed final state $\mathrm{c\bar{s}}\tau^-\bar{\nu}_\tau$ is characterized by two jets originating from the hadronic decay of one of the charged Higgs bosons and a τ jet with missing energy due to the prompt neutrino as well as to the neutrino(s) from the subsequent τ decay.

The preselection is the same as that described in Ref. [3]. In order to identify the τ jet an algorithm based on "minijets" is used as described in Ref. [16]. If a minijet satisfies the τ-jet selection criteria, the rest of the event is clustered into two jets using the Durham [17] clustering algorithm. A kinematic fit is performed with the constraints of energy and momentum conservation and equality of the $\mathrm{c\bar{s}}$ and $\tau^+\nu_\tau$ masses. If there is more than one τ candidate the combination with the lowest χ^2 is taken.

Table 2: The signal event selection efficiencies ϵ (in %), parametrized as a function of the charged Higgs boson mass $m_{\mathrm{H}^\pm}$, at $\sqrt{s}$= 206 GeV.

$m_{\mathrm{H}^\pm}(\mathrm{GeV}/c^2)$	60	65	70	75	80	85	90
ϵ $(\tau^+\nu_\tau\tau^-\bar{\nu}_\tau)$	24.4	25.5	26.4	27.3	28.0	28.5	28.9
ϵ $(\mathrm{c\bar{s}}\tau^-\bar{\nu}_\tau)$	49.1	48.0	45.8	42.8	38.8	33.9	28.0
ϵ $(\mathrm{c\bar{s}s\bar{c}})$	60.7	62.9	64.5	65.5	66.1	66.3	66.3

Table 3: Numbers of candidate events and background expected from Standard Model processes, for each of the three years of data taking.

Channel	$\sqrt{s}$ (GeV)	observed events	expected background
$\tau^+\nu_\tau\tau^-\bar{\nu}_\tau$	188.6	14	11.0
	192-202	22	15.6
	204-209	9	14.0
$\mathrm{c\bar{s}}\tau^-\bar{\nu}_\tau$	188.6	63	67.3
	192-202	89	113.1
	204-209	127	108.9
$\mathrm{c\bar{s}s\bar{c}}$	188.6	778	826.3
	192-202	1034	1102.6
	204-209	950	963.2

In order to reject background from $\mathrm{W^+W^-} \to (\mathrm{e}/\mu)\nu\mathrm{q\bar{q}}'$, the measured energy of the τ jet boosted into the Higgs rest frame is required to be less than $0.175\sqrt{s}$. The boost is performed using the information from the hadronic side of the event.

After this procedure the following four variables are chosen to further suppress the background:

- the total missing transverse momentum of the event, P_T^{miss};
- the isolation angle θ_{iso} of the τ, defined as the half-angle of the cone around the τ jet direction containing 5% of the total energy of the rest of the event;
- the χ^2 from the kinematic fit;
- the decay angle $\theta_\tau^{\mathrm{ch}}$, defined as the angle between the τ momentum in the Higgs boson centre-of-mass frame and the Higgs boson flight direction, charge-tagged with the charge of the τ, to exploit the asymmetry in the W system, absent for scalars.

The four variables are linearly combined into one variable, D_1, defined as

$$D_1 \;=\; 0.021\; P_T^{\mathrm{miss}} \;+\; 0.400\; \theta_{\mathrm{iso}} \;-\; 0.058\; \chi^2 \;-\; 0.148\; \theta_\tau^{\mathrm{ch}} \;-\; 0.881$$

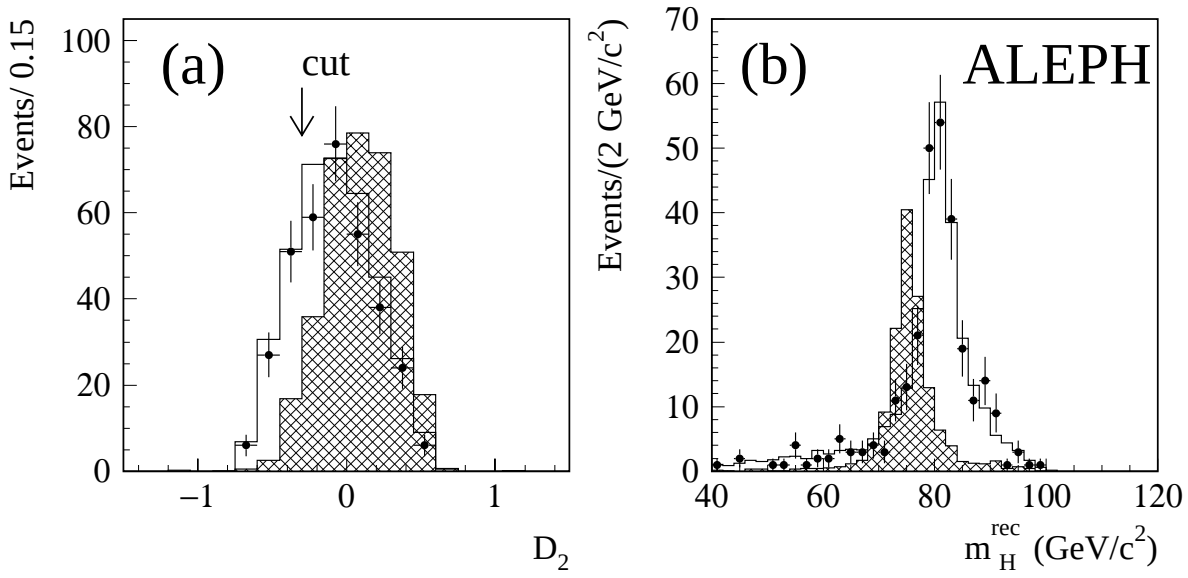

Figure 2: (a) The distribution of the discriminant variable D_2 described in the text for the semi-leptonic channel. (b) The distribution of the fitted mass of the Higgs boson candidates after the cut on D_2. The points are the data, the open histogram is the Standard Model background and the hatched histogram represents the Higgs boson signal expectation with $m_{\mathrm{H}^\pm} = 75\,\mathrm{GeV}/c^2$. The signal is arbitrarily normalized.

where P_T^{miss} is in GeV/c, and θ_{iso} and $\theta_\tau^{\mathrm{ch}}$ are in radians. Events are selected by requiring that $D_1 > -0.1$. The background consists primarily of $\mathrm{W^+W^-} \to \ell\nu\mathrm{q\bar{q}}'$ events.

Due to the scalar nature of the $\mathrm{H^+}$, the τ^+ from its decay is produced in a left-handed helicity state, in contrast to the τ^+'s from $\mathrm{W^+}$ decays. Variables designed for the measurement of the τ polarization at LEP 1 [18] have been used to form an event-by-event helicity estimator, $\mathcal{E}_\tau$. This variable, together with the charge-tagged production angle $\theta_{\mathrm{prod}}^{\mathrm{ch}}$ [3], is used to discriminate further between $\mathrm{W^+W^-} \to \tau\nu\mathrm{q\bar{q}}'$ and $\mathrm{H^+H^-} \to \mathrm{c\bar{s}\tau^-\bar{\nu}_\tau}$ events. The two variables are combined into another variable, D_2, defined as

$$D_2 \;=\; -\,0.461\;\theta_{\mathrm{prod}}^{\mathrm{ch}} \;-\; 0.517\;\mathcal{E}_\tau \;+\; 1.020\;,$$

where $\theta_{\mathrm{prod}}^{\mathrm{ch}}$ is expressed in radians. The distribution of D_2 is shown in Fig. 2a. The cut optimization yields $D_2 > -0.3$ for $m_{\mathrm{H}^\pm}$=75 GeV/c^2. The selection efficiencies are given in Table 2 as a function of the Higgs boson mass for $\sqrt{s} = 206\,\mathrm{GeV}$. They are only weakly dependent on $\sqrt{s}$. In the data collected between $\sqrt{s} = 189$ and 209 GeV, the numbers of selected events are compared with the background expectations in Table 3. The fitted-mass distribution of the Higgs boson candidates is shown in Fig. 2b. For $m_{\mathrm{H}^\pm}$=77 GeV/c^2, close to the sensitivity of this search, and for $\mathrm{B(H^+ \to \tau^+\nu_\tau)}$=0.5, a total of 21.2 signal events is expected.

The systematic uncertainty on the number of expected signal events is estimated to be 3.0%. The main contributions are the finite size of the simulated event samples (2.2%),

calorimeter calibration uncertainties (0.5%) and the uncertainty on the cross section for charged Higgs boson production (2%). The systematic error on the background level was estimated to be 3.9%. The main contributions are from limited statistics of the simulated event samples (2.5%), uncertainty on the cross section for the W^+W^- process (0.5%) and calibration uncertainties (3%).

3.3 The $c\bar{s}s\bar{c}$ final state

The hadronic decays of pair-produced charged Higgs bosons lead to a four-jet final state with equal mass dijet systems. The preselection remains unchanged with respect to Ref. [3].

A five-constraint kinematic fit is performed with energy-momentum conservation and equal dijet-mass constraints. In this fitting procedure, the errors on the jet energies and angles are parametrized as for the W mass measurement in the four-jet channel [19]. The pairing is chosen as the dijet combination giving the minimum χ^2.

To evaluate the mass difference between the two dijet invariant masses, momentum and energy conservation is imposed to rescale the energies of the four jets, fixing the jet velocities at their measured values. The mass difference Δm between the two rescaled dijets is required to be smaller than $30\,\mathrm{GeV}/c^2$.

To improve the background rejection a linear discriminant D_3 is constructed, combining the following five variables:

- the production polar angle θ_{prod}, *i.e.* the angle between the Higgs boson momentum direction and the beam axis;
- the difference Δm between the two rescaled dijet masses;
- the χ^2 of the 5C kinematic fit;
- the product of the minimum jet energy E_{min} and the minimum jet-jet angle $\theta_{\mathrm{q\bar{q}}}$;
- the logarithm of the QCD four-jet matrix element squared $\mathcal{M}_{\mathrm{QCD}}$ [20].

The optimized LDA coefficients were determined at $\sqrt{s} = 206$ GeV with a cocktail of five charged Higgs boson masses ranging between 80 and 88 GeV/c^2, leading to:

$$\begin{aligned} D_3 \;=\; & -\,0.951\;\cos^2\theta_{\mathrm{prod}} \;-\; 0.0065\;\Delta m \;-\; 0.000968\;\chi^2_{5\mathrm{C}} \\ & -\,0.0034\;(E_{\mathrm{min}} \times \theta_{\mathrm{q\bar{q}}}) \;-\; 0.335\;\log_{10}(\mathcal{M}_{\mathrm{QCD}})\;, \end{aligned}$$

with Δm in GeV/c^2, E_{min} in GeV, $\theta_{\mathrm{q\bar{q}}}$ in radians, and $\mathcal{M}_{\mathrm{QCD}}$ in GeV^{-4}. The distribution of D_3 is shown in Fig. 3a. The cut was optimized for $m_{\mathrm{H}^\pm}$=76, 80 and $84\,\mathrm{GeV}/c^2$. Events are accepted if $D_3 > 1.3$. For $m_{\mathrm{H}^\pm}$=$75\,\mathrm{GeV}/c^2$ and $\mathrm{B}(\mathrm{H}^+ \to \tau^+\nu_\tau)$=0, a total of 101.9 events is expected in the data. The efficiency does not depend on $\sqrt{s}$.

After the complete selection, the comparison between data and simulation is displayed in Fig. 3b for the dijet invariant mass. The numbers of events observed in the data are

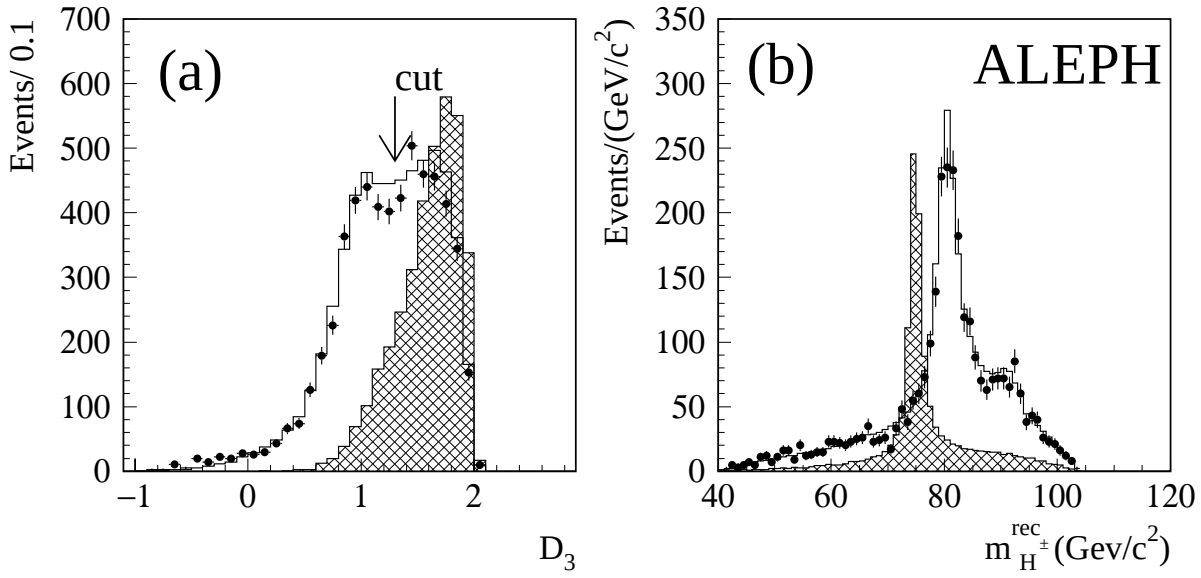

Figure 3: (a) The distribution of the discriminating variable D_3. (b) The distribution of the reconstructed mass of the Higgs boson candidates after the cut on the discriminating variable. The points are the data, the open histograms are the Standard Model backgrounds and the hatched histogram represents the Higgs signal expectation for $m_{\mathrm{H}^\pm} = 75\,\mathrm{GeV}/c^2$. The signal is arbitrarily normalized.

compared in Table 3 to the expected background from Standard Model processes, dominated by $\mathrm{W}^+\mathrm{W}^-$ production. An overall 2.4 standard deviation deficit with respect to expectation is observed. It is correlated with the deficit observed in the measurement of the $\mathrm{W}^+\mathrm{W}^-$ hadronic cross section [12], which was ascribed to a statistical fluctuation.

The systematic error on the number of expected signal events is estimated to be 2.5%. The main contributions are from limited sample statistics (1.3%), uncertainty on the cross section for charged Higgs production (2%) and accuracy of the simulation (0.5%). The systematic error on the expected background, dominated by $\mathrm{W}^+\mathrm{W}^-$ and $\mathrm{q\bar{q}}$ production, is estimated to be 2.0%. The main contributions are from the simulated sample statistics (0.4% for $\mathrm{W}^+\mathrm{W}^-$ and 1.6% for $\mathrm{q\bar{q}}$), the uncertainty on the cross section (0.5% for $\mathrm{W}^+\mathrm{W}^-$ and 5% for $\mathrm{q\bar{q}}$), and the adequacy of the simulation (1.4% for $\mathrm{W}^+\mathrm{W}^-$ and 2.1% for $\mathrm{q\bar{q}}$).

4 Results

No evidence for a signal is observed in the data. The results of the three selections have been combined to set a 95% C.L. lower limit on the mass of charged Higgs bosons.

Full background subtraction has been performed in setting the limit with the likelihood ratio test statistic [21]. Systematic uncertainties are taken into account according to Ref. [22]. To improve the sensitivity of the analysis, the charged Higgs boson mass has

been used as a discriminating variable for the $c\bar{s}s\bar{c}$ and $c\bar{s}\tau^-\bar{\nu}_\tau$ channels. In the previous publications [1, 2, 3], only event counting was used in the $\tau^+\nu_\tau\tau^-\bar{\nu}_\tau$ channel. In this analysis, the discriminant variable D_0 has been introduced in the limit setting procedure.

The result of the combination of the three analyses is shown in Fig. 4. Charged Higgs bosons with mass lower than $79.3\,\mathrm{GeV}/c^2$ are excluded at the 95% C.L. independently of $\mathrm{B}(\mathrm{H}^+\to\tau^+\nu_\tau)$. The corresponding expected exclusion is $77.1\,\mathrm{GeV}/c^2$. For the values $\mathrm{B}(\mathrm{H}^+\to\tau^+\nu_\tau) = 0$ and 1, 95% C.L. lower limits on $m_{\mathrm{H}^\pm}$ are set at $80.4\,\mathrm{GeV}/c^2$ (with $78.2\,\mathrm{GeV}/c^2$ expected) and $87.8\,\mathrm{GeV}/c^2$ (with $89.2\,\mathrm{GeV}/c^2$ expected) respectively.

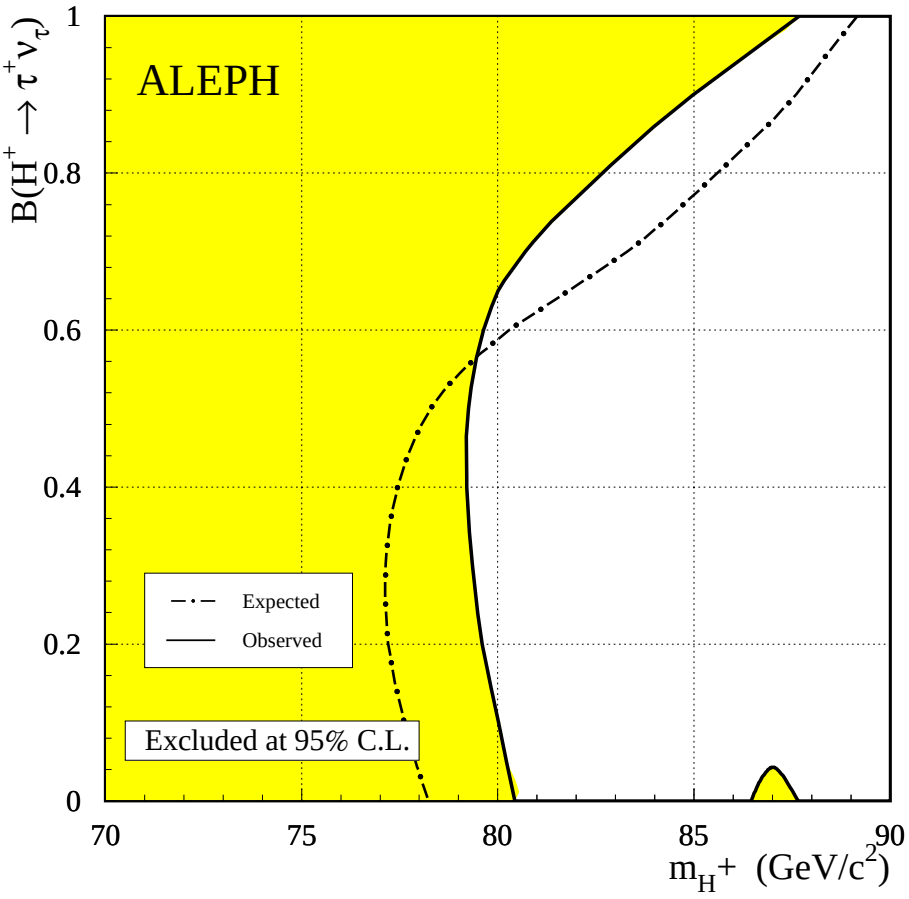

Figure 4: Limit at 95% C.L. on the charged Higgs boson mass as a function of $\mathrm{B}(\mathrm{H}^+\to\tau^+\nu_\tau)$. The expected (dash-dotted) and observed (solid) exclusion curves are shown for the combination of the three analyses, using the full 189–209 GeV data set.

Upper limits can also be derived on the $\mathrm{H}^+\mathrm{H}^-$ cross section at $\sqrt{s} = 200\,\mathrm{GeV}$, as a function of the Higgs boson mass, for $\mathrm{B}(\mathrm{H}^+\to\tau^+\nu_\tau)$=0, 50 and 100%. To combine the data at different centre-of-mass energies, the limit on the cross section was extrapolated to 200 GeV with the expected $\sqrt{s}$ dependence for the production of a charged scalar particle pair. The result is shown in Fig. 5 as a function of $m_{\mathrm{H}^\pm}$.

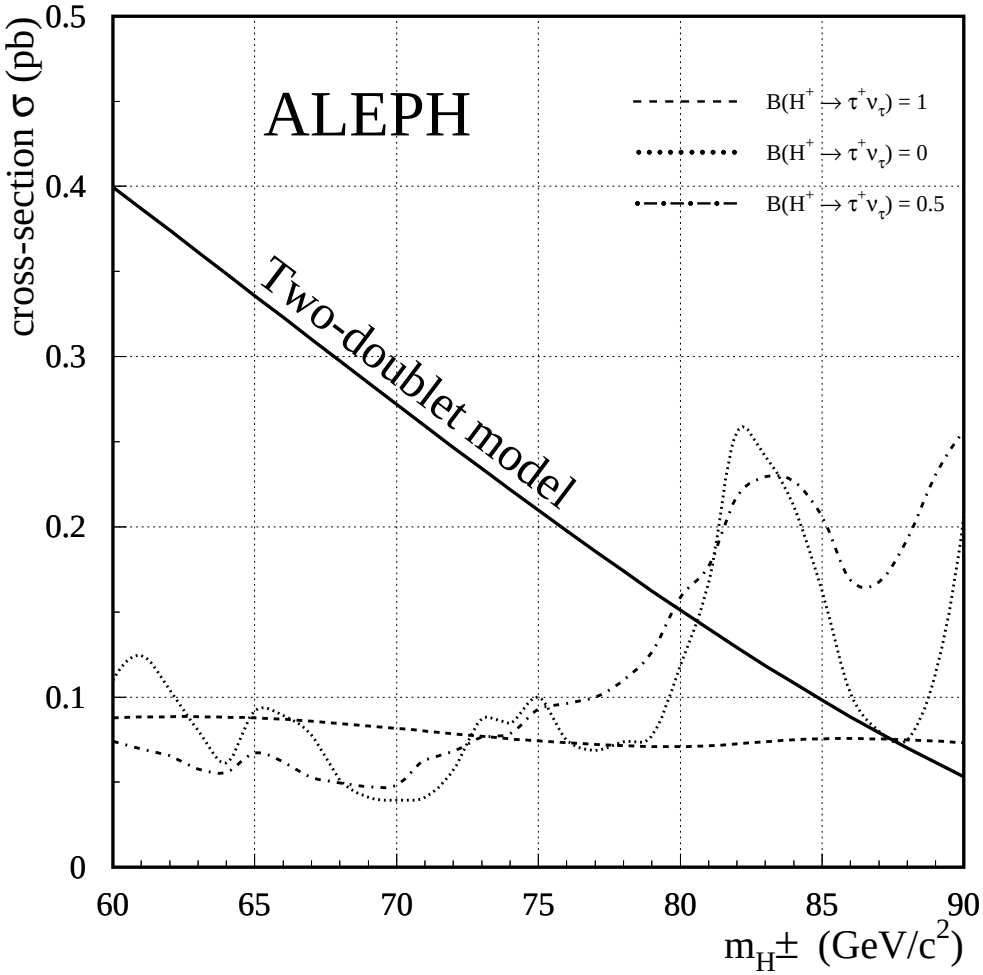

Figure 5: Upper limits at 95% C.L. on the H^+H^- production cross section at $\sqrt{s} = 200$ GeV for $B(H^+ \to \tau^+\nu_\tau)$=1 (dashed line), $B(H^+ \to \tau^+\nu_\tau)$=0 (dotted line) and $B(H^+ \to \tau^+\nu_\tau)$=0.5 (dashed-dotted line). The charged Higgs boson production cross section in the two-Higgs-doublet model is shown as a solid curve.

5 Conclusions

Pair-produced charged Higgs bosons have been searched for in the three final states $\tau^+\nu_\tau\tau^-\bar{\nu}_\tau$, $c\bar{s}\tau^-\bar{\nu}_\tau$ and $c\bar{s}s\bar{c}$, with 629 pb^{-1} of data collected at centre-of-mass energies from 189 to 209 GeV. No evidence for Higgs boson production was found and lower limits were set on $m_{H^\pm}$ as a function of $B(H^+ \to \tau^+\nu_\tau)$, within the framework of two-Higgs-doublet models. Assuming $B(H^+ \to \tau^+\nu_\tau)+B(H^+ \to c\bar{s})=1$, charged Higgs bosons with mass below 79.3 GeV/c^2 are excluded at 95% C.L., independent of $B(H^+ \to \tau^+\nu_\tau)$.

Acknowledgements

It is a pleasure to congratulate our colleagues from the accelerator divisions for the successful operation of LEP at high energy. We are indebted to the engineers and technicians in all our institutions for their contribution to the excellent performance of ALEPH. Those of us from non-member states wish to thank CERN for its hospitality and support.

References

[1] ALEPH Collaboration, *"Search for charged Higgs bosons in e^+e^- collisions at centre-of-mass energies from 130 to 172 GeV"*, Phys. Lett. **B418** (1998) 419.

[2] ALEPH Collaboration, *"Search for charged Higgs bosons in e^+e^- collisions at $\sqrt{s}$ = 181-184 GeV"*, Phys. Lett. **B450** (1999) 467.

[3] ALEPH Collaboration, *"Search for charged Higgs bosons in e^+e^- collisions at $\sqrt{s}$ = 189 GeV"*, Phys. Lett. **B487** (2000) 253.

[4] DELPHI Collaboration, *"Search for Charged Higgs at LEP2"*, Phys. Lett. **B460** (1999) 484;
L3 Collaboration, *"Search for charged Higgs bosons in e^+e^- collisions at centre-of-mass energies up to 202 GeV"*, Phys. Lett. **B496** (2000) 34;
OPAL Collaboration, *" Search for Higgs bosons in e^+e^- collisions at 183 GeV"*, Eur. Phys. J. **C7** (1999) 407;
CDF Collaboration, *"Search for the Charged Higgs Bosons in the Decay of Top Quark Pairs in the $e\tau$ and $\mu\tau$ Channels at $\sqrt{s}$ = 1.8 TeV"*, Phys. Rev. **D62** (2000) 012004;
D0 Collaboration, *"Direct Search for Charged Higgs Bosons in Decays of Top Quarks"*, FERMILAB-Pub-01/022-E, hep-ex/0102039, submitted to Phys. Rev. Lett..

[5] ALEPH Collaboration, *"ALEPH: a detector for electron-positron annihilations at LEP"*, Nucl. Instrum. and Methods **A294** (1990) 121;
D. Creanza *et al.*, *The new ALEPH silicon vertex detector*, Nucl. Instrum. and Methods **A409** (1998) 157.

[6] ALEPH Collaboration, *"Performance of the ALEPH detector at LEP"*, Nucl. Instrum. and Methods **A360** (1995) 481.

[7] S. Jadach, B.F.L. Ward, and Z. Wąs, *"The Monte Carlo program KORALZ, version 4.0, for the lepton or quark pair production at LEP/SLC energies"*, Comput. Phys. Commun. **79** (1994) 503.

[8] M. Skrzypek, S. Jadach, W. Placzek and Z. Wąs, *"Monte Carlo program KORALW-1.02 for W pair production at LEP-2/NLC energies with Yennie-Frautschi-Suura exponentiation"* Comput. Phys. Commun. **94** (1996) 216.

[9] T. Sjöstrand, *"The PYTHIA 5.7 and JETSET 7.4 Manual"*, LU-TP 95/20, CERN-TH 7112/93, Comput. Phys. Commun. **82** (1994) 74.

[10] A. Denner, S. Dittmaier, M. Roth and D. Waeckeroth, Phys. Lett. **B475** (2000) 127.

[11] S. Jadach, W. Płaczek, M. Skrzypek and B. F. L. Ward, Phys. Rev. **D54** (1996) 5434;
S. Jadach, W. Płaczek, M. Skrzypek, B. F. L. Ward and Z. Wąs, Phys. Lett. **B417** (1998) 326;
S. Jadach, W. Płaczek, M. Skrzypek, B. F. L. Ward and Z. Wąs, *"Final State Radiative Effects for the Exact O(α) YFS Exponentiated (Un)Stable* W^+W^- *Production at and beyond LEP2 Energies"*, Phys. Rev. **D61** (2000) 113010.

[12] ALEPH Collaboration, *"Measurement of W-pair production in* e^+e^- *collisions at* $\sqrt{s}$*=189 GeV"*, Phys. Lett. **B484** (2000) 205.

[13] J. A. M. Vermasaeren in *Proceedings of the IVth international workshop on gamma-gamma interactions*, Eds. G. Cochard and P. Kessler, Springer Verlag, 1980.
S. Kawabata, presented by J. H. Field in *Proceedings of the IVth international colloquium on photon-photon interactions* (Paris 1981) p. 447.

[14] G. Ganis and P. Janot, *"The HZHA Generator"* in *"Physics at LEP2"*, Eds. G. Altarelli, T. Sjöstrand and F. Zwirner, CERN 96-01 (1996), Vol. 2, 309.

[15] JADE Collaboration, *"Experimental investigation of the energy dependence of the strong coupling strength"*, Phys. Lett. **B213** (1988) 235.

[16] ALEPH collaboration, *"Searches for the Neutral Higgs bosons of the MSSM in* e^+e^- *collisions at centre-of-mass energies of 181-184 GeV"*, Phys. Lett. **B440** (1998) 419.

[17] W. J. Stirling, *"Hard QCD Working Group - Theory Summary"*, J. Phys. **G17** (1991) 1567.

[18] M. Davier, L. Duflot, F. Le Diberder, A. Rougé, *"The optimal method for the measurement of tau polarisation"*, Phys. Lett. **B306** (1993) 411.

[19] ALEPH Collaboration, *"Measurement of the W mass by direct reconstruction in* e^+e^- *collisions at 172 GeV"*, Phys. Lett. **B422** (1998) 384.

[20] D. Danckaert, P. De Causmaecker, R. Gastmans, W. Troost, T. T. Wu, *"Four-jet production in* e^+e^- *annihilation"*, Phys. Lett. **B114** (1982) 203.

[21] W. T. Eadie *et al.*, *"Statistical Methods in Experimental Physics"*, North-Holland Publishing Company, 1971.

[22] R. D. Cousins and V. L. Highland, *"Incorporating systematic uncertainties into an upper limit"*, Nucl. Instrum. and Methods **A320** (1992) 331.